DOI 10.1007/s10812-017-0427-1
Journal of Applied Spectroscopy, Vol. 84, No.1, March, 2017 (Russian Original Vol. 84, No. 1, January–February, 2017)

A STUDY OF THE OPTICAL PROPERTIES OF BARIUM SELENIDE CRYSTALS. I. FUNDAMENTAL FUNCTIONS

V. V. Sobolev,[a*] D. A. Merzlyakov,[a] V. Val. Sobolev[a,b]

UDC 535.33; 546.431; 661.844

The full complex of 18 fundamental optical functions describing a barium selenide crystal was obtained in the spectral range of 0–40 eV. Their main features and general laws were established. Calculations were performed using a series of computer programs based on the Kramers–Kronig integral relations, the Taft–Philippe extrapolation model, and experimental reflectance spectra in the regions of 3.0–5.5 eV at 2 K and 3–40 eV at 77 K.

Keywords: *barium selenide, optical function, maximum, shoulder, exciton, interband transition, plasmon.*

Introduction. Chalcogenides of Group II*A*-VI alkaline earth elements play an important role in technological methods of semiconductor optoelectronics, catalytic processes, in manufacturing of efficient luminophores, etc. [1, 2]. Barium selenide (BaSe) stands out among them as the compound with the lowest energy band gap. Its most long-wavelength excitonic maximum of optical density $D = \alpha d$ for films at 77 K was determined to be ~3.6 eV [3, 4]. The most accurate reflection spectra of BaSe are obtained by analyzing cleaved single crystals at 2 K in the 3.0–5.5 eV range and at 77 K in the 3–40 eV range [5, 6]. It is estimated [5], under the assumption that the binding energy of the long-wavelength exciton is $E_x \cong 0.08$ eV, that the lowest direct interband transition energies for BaSe at points X and Γ of the Brillouin zone (BZ) are $E_{gd}(X) = 3.66$ and $E_{gd}(\Gamma) = 4.56$ eV, and the energy of indirect transitions is $E_{gi}(X–\Gamma) \cong 3.42$ eV. Barium selenide crystallizes in a NaCl-type cubic lattice. The refractive index of BaSe in the transparent wavelength region is $n_\infty \cong 2.11$ [7], i.e., $\varepsilon_\infty \cong 4.41$. From the analysis of variance (ANOVA) of the IR reflection spectrum of a BaSe single crystal in the 0–300 cm^{-1} range the static dielectric constant was determined to be $\varepsilon_0 = 10.7$ [7, 8]. Very narrow intense peaks at about 3.58, 3.91 eV and less intense peaks at about 4.52 and 4.95 eV [5], previously [3, 4] observed in optical density spectra of BaSe films, were observed in the reflection spectrum of a single crystal at 2 K in the 3.0–5.5 eV range.

Electronic structure of BaSe was studied in greatest detail by the full-potential linearized augmented-planewave (FP-LAPW) [9] method. Spin–orbit interaction splits the topmost valence band of BaSe into about 0.41 and 0.32 eV at the points Γ and X. The third valence band at the point X is about 0.5 eV below the topmost. Indirect transitions from $E_{gi}(\Gamma–X) \cong 2.1$ eV are forbidden by symmetry. At points X and Γ the bottom conduction band minima are singlet and triplet, and the distance between them is $\Delta E_{1,2} \cong 0.4$, $\Delta E_{1,3} \cong 0.85$ eV. In [9] the $\varepsilon_2(E)$, $\varepsilon_1(E)$, $\alpha(E)$, $-\mathrm{Im}\,\varepsilon^{-1}$, and $R(E)$ spectra were calculated in the 0–25 eV range. In [10] BaSe zones were determined by combining the Kohn–Sham model with the generalized gradient approximation (KS-GGA) and by the many-particle approximation (G_0W_0) excluding Δ_{CO}. In the second case the energies $E_{gd}(X)$ and $E_{gd}(\Gamma)$ were almost as high as in experimental evaluation [5]. These calculations were continued using the two-particle Green's function and the Bethe–Salpeter equation (BSE), as well as in combination with the G_0W_0 approximation (BSE-G_0W_0) for the spectrum $\varepsilon_2(E)$ in the 2–4.3 eV range. The theoretical [10] triplet (BSE-G_0W_0) and quartet (BSE) of the bands strongly differ from the experimental data [5] in distribution on the energy scale and in intensity. This is due to neglecting spin-orbital splitting of the upper valence band of BaSe, which determines all the features of the long-wavelength structures. The fundamental result of the calculations [9] is the prediction of a very complex structure of two broad barium selenide $\varepsilon_2(E)$ bands in the 3– 2 and 12– 5 eV ranges. However, there is no data on the energy maxima of the bands and their intensities, and estimated long-wave $\varepsilon_2(E)$ spectra taking into account excitons are highly contradictory. It should also be noted that the inclusion of excitons in a broad energy range can significantly distort the entire structure of the transition bands and their intensities [11].

*To whom correspondence should be addressed.

[a]Udmurt State University, 1 Universitetskaya Str., Izhevsk, 426034, Russia; e-mail: sobolev@uni.udm.ru; [b]M. T. Kalashnikov Izhevsk State Technical University, Izhevsk, Russia. Translated from Zhurnal Prikladnoi Spektroskopii, Vol. 84, No. 1, pp. 72–78, January–February, 2017. Original article submitted August 22, 2016.

At the beginning of the history of theoretical calculations the natural fundamental assumption was made that the electronic structure of crystals is determined by the features of the structure and symmetry of the crystal lattice and the Brillouin zone, i.e. it must become more complicated with the transition from simple cubic lattices to the more complex. This was evidenced by the relatively simple form and similarities of the energy bands of diamond-like compounds of the A^{IV}, $A^{III}B^{V}$, and $A^{II}B^{VI}$ groups despite great differences in their ionic character [12, 13]. However, the transition to isoelectronic chalcogenides of the II*A*-VI group with a different though very simple NaCl-type cubic lattice led to a radical restructuring of the entire electronic spectrum in a wide energy range from the long-wave absorption edge up to about 40 eV [5, 6], more significant than in cubic crystals of the $A^{I}B^{VII}$ group [13]. The nature of this very strong difference in the electronic structure of group II-VI and II*A*-VI compounds is not clear. This is due to scarcity of information for crystals of the II*A*-VI group.

The purpose of this work is to obtain new quantitative information in the 0– 0 eV range about spectral features of 18 fundamental optical functions and the electronic structure of barium selenide.

Calculation Methods. It is generally accepted to study the electronic structure by various spectroscopic methods, and 18 optical functions contain the most complete and detailed information [12–16]: the reflection $R(E)$ and absorption $\alpha(E)$ coefficients; indices of refraction $n(E)$ and absorption $k(E)$; real $\varepsilon_1(E)$ and imaginary $\varepsilon_2(E)$ components of the transverse dielectric function $\varepsilon(E)$; real Re ε^{-1}, Re $(1 + \varepsilon)^{-1}$ and imaginary –Im ε^{-1}, –Im $(1 + \varepsilon)^{-1}$ components of the longitudinal dielectric functions ε^{-1}, $(1 + \varepsilon)^{-1}$; combined density of states $E^2\varepsilon_2(E)$ with a constant probability of transitions; an effective number of valence transitions n_{eff} involved in transitions to a given energy E, which can be calculated from the spectra of $\varepsilon_2(E)$, $k(E)$, –Im ε^{-1}, and –Im $(1 + \varepsilon)^{-1}$; effective dielectric constant $\varepsilon_{\text{eff}}(E)$; optical conductivity $\sigma(E)$, and others.

In a wide energy range only $R(E)$ is experimentally determined, and the functions of bulk (–Im ε^{-1}) and surface (–Im $(1 + \varepsilon)^{-1}$) characteristic electron energy losses are extracted from the integral energy loss function using very complex and approximate techniques. In addition, sometimes $\varepsilon_1(E)$ and $\varepsilon_2(E)$ are measured in the E_{gd}–5.5 eV range by ellipsometric methods. For the BaSe crystal only reflectance spectra are known.

Calculations of the 18 functions were performed using computer programs written on the basis of the Kramers–Kronig integral relations and analytical formulas of correlation between functions. The Taft–Philippe extrapolation model was used for the extrapolation of $R(E)$ in the energy range of $E > 40$ eV, and in the transparency region of $E < E_g$ the $R(E)$ coefficient was determined from the experimental value of the dielectric constant [7]. Useful techniques are described in [12–16] and were used repeatedly in [17–20].

Results and Discussion. Calculations of 18 optical functions were performed in the 0–40 eV range, while n_{eff} was determined in the 3–60 eV range using experimental reflection spectra at 2 K in the 3.5–5.5 eV range and at 77 K in the 3–40 eV range [5, 6]. According to estimates based on $n(E < 2 \text{ eV}) \cong 2.1$ [7], the reflection coefficient of BaSe in the transparency region is $R(E < 2 \text{ eV}) \approx 0.126$. In the unmeasured energy region $E > 40$ eV it was chosen by the Taft–Philippe extrapolation method [12] using the sum rule for $n(E)$.

Calculation results can be conveniently discussed in three energy ranges: 3.0–5.5, 5.5–13.0, 0–40 eV, and for the ε^{-1}, $(1 + \varepsilon)^{-1}$ spectra the 0–60 eV range is also considered (Fig. 1, Table 1). The experimental reflectance spectrum of $R(E)$ at 2 K in the 3.0–5.5 eV range contains a dispersion structure defined by a sharp peak 1 and a sharp valley at about 3.605 eV, two dispersion structures with peaks 3 and 6, the peak 8, and weakly expressed shoulders 2, 4, 5, 7 (Fig. 1a). The calculated curves $\varepsilon_1(E)$ and $n(E)$ repeat the shape of $R(E)$ of the first three bands, and for the fourth band are transformed into a weakly pronounced peak. The $\varepsilon_1(E)$ and $n(E)$ peaks are offset relative to the $R(E)$ peaks to lower energies by 0.01–0.03 (ε_1) and 0.01–0.02 eV (n).

The $\boldsymbol{\varepsilon}_2(E)$, $k(E)$, $\alpha(E)$, $E^2\varepsilon_2(E)$, and $\sigma(E)$ spectra are very similar in shape (Fig. 1d). Intensities and half-widths of the bands 1 and 6 are much lower than of 3 and 8. The shoulder *2* of reflection, $n(E)$, $\varepsilon_1(E)$ is transformed into a peak in the $\varepsilon_2(E)$, $k(E)$, $\alpha(E)$, $E^2\varepsilon_2(E)$ and $\sigma(E)$ spectra. Peak intensities of four bands are about 13, 10, 8, and 5 (ε_2), 2.2, 1.5, 1.2 and 1.1 (k), $8{\cdot}10^5$, $6{\cdot}10^5$, $6{\cdot}10^5$, and $5.8{\cdot}10^5$ cm^{-1} (α), 160, 140, 150, and 140 ($E^2\varepsilon_2$), $5{\cdot}10^{15}$, $4.4{\cdot}10^{15}$, $2.8{\cdot}10^{15}$, and $2.7{\cdot}10^{15}$ s^{-1} (σ). In a simplified interpolation of a continuous spectrum under the bands of a monotonic curve, intensities of these four peaks of the five functions markedly decrease, especially for the shortwave region.

Longitudinal functions of bulk (–Im ε^{-1}) and surface (–Im $(1 + \varepsilon)^{-1}$) electron energy losses in the 3.5–5.5 eV range are very similar (Fig. 1g) when peak intensities of the four bands of surface losses are decreased about 1.2–1.4 times relative to –Im ε^{-1}. Energies of longitudinal-transverse splitting are $\Delta E_{lt} = E_i(-\text{Im } \varepsilon^{-1}) - E_i(\varepsilon_2) \cong 0.01$–$0.04$ eV, and the difference between the peak energies of bulk and surface electron energy losses is ≤0.01 eV. The spectra Re ε^{-1} and Re $(1 + \varepsilon)^{-1}$ are in the form of dispersion curves in place of four peaks in –Im ε^{-1} and –Im $(1 + \varepsilon)^{-1}$ (Fig. 1j).

It is interesting to consider the features of the $n_{\text{eff}}(E)$ spectra calculated on the basis of the functions $\varepsilon_2(E)$, $k(E)$, –Im ε^{-1}, and Im $(1 + \varepsilon)^{-1}$. These features are due to different effects: ε_2 — dissipation of energy of the incident electromagnetic

TABLE 1. Peak and Shoulder (in Parentheses) Energies (Ev) of the Optical Functions of Base

No.	R	ε_1	n	σ	ε_2	k	α	$\varepsilon_2 E^2$	$-\mathrm{Im}\,\varepsilon^{-1}$	$-\mathrm{Im}\,(1+\varepsilon)^{-1}$	$\mathrm{Re}\,\varepsilon^{-1}$	$\mathrm{Re}\,(1+\varepsilon)^{-1}$
2	3.58	3.55	3.56	3.58	3.58	3.58	3.58	3.58	3.60	3.59	3.59	3.59
3	(3.69)	(3.69)	(3.69)	3.72	3.72	3.72	3.72	3.72	3.73	3.72	3.71	3.71
4	3.91	3.89	3.90	3.91	3.91	3.91	3.91	3.91	3.95	3.95	3.99	3.99
5	(4.04)	(4.04)	(4.04)	(4.04)	(4.04)	(4.04)	(4.04)	(4.04)	(4.04)	(4.04)	–	–
6	(4.40)	(4.39)	(4.40)	(4.40)	(4.40)	(4.42)	(4.42)	(4.40)	4.42	4.42	4.42	4.42
7	4.52	4.51	4.51	4.52	4.52	4.52	4.52	4.52	4.53	4.53	4.55	4.55
8	(4.63)	(4.60)	(4.60)	(4.63)	(4.61)	(4.63)	(4.61)	(4.63)	–	–	–	–
9	4.96	(4.94)	4.94	4.96	4.96	4.97	4.97	4.98	4.99	4.98	–	–
10	6.35	6.05	6.18	6.35	6.35	6.35	6.35	6.35	6.40	6.40	(6.40)	(6.40)
11	6.81	(6.61)	(6.61)	6.81	6.81	6.81	6.81	6.81	(7.00)	(6.97)	–	–
12	8.48	(7.96)	(8.03)	8.14	8.14	8.40	8.40	8.24	(7.80)	(7.80)	(7.80)	(7.80)
13	9.57	9.10	(9.15)	(9.15)	(9.15)	9.21	9.26	(9.15)	9.10	(9.10)	(9.10)	(9.10)
14	10.14	10.04	10.04	10.04	10.04	10.09	10.09	10.04	10.04	9.98	(10.00)	(10.00)
15	(11.50)	(10.70)	(10.70)	(10.30)	(11.30)	(11.30)	(11.30)	(11.30)	–	(11.50)	–	–
16	12.02	11.24	11.30	11.70	(11.80)	11.80	11.80	11.80	12.21	12.02	12.45	12.22
17	(12.80)	(12.48)	12.64	12.64	12.64	12.64	12.64	12.64	12.88	(12.85)	12.90	12.85
18	(14.20)	(13.94)	(13.94)	(14.11)	(14.11)	(14.20)	(14.20)	(14.11)	14.20	(14.20)	–	–
19	14.77	(14.58)	14.58	14.77	14.77	14.77	14.77	14.77	14.77	14.77	15.00	15.00
20	16.54	15.50	15.90	16.18	16.18	16.33	16.54	16.33	17.01	16.80	17.30	17.30
21	19.04	17.58	18.03	18.38	18.23	18.52	18.85	18.52	19.50	19.04	19.50	19.50
22	21.95	19.77	19.95	20.46	20.35	20.81	20.81	20.60	22.37		22.35	22.10
23	(23.20)	(22.68)	22.58	(22.89)	(22.89)	(22.89)	(22.89)	(22.89)	–	23.04	–	–
E_{p1}	–	–	–	–	–	–	–	–	10.74	10.14	11.20	10.50
E_{p2}	–	–	–	–	–	–	–	–	23.30	21.30	26.40	23.30

wave, k – attenuation of its amplitude, $-\mathrm{Im}\,\varepsilon^{-1}$ and $-\mathrm{Im}\,(1+\varepsilon)^{-1}$ — bulk and surface energy losses of fast charged particles. At high frequencies $n_{\mathrm{eff}}(E)$ are the same and equal to the number of valence electrons. With increasing energy in the 3.5–5.5 eV range they have almost the same shape. The curve of $n_{\mathrm{eff}}(-\mathrm{Im}\,\varepsilon^{-1})$ is ~1.6 times greater than $-\mathrm{Im}\,(1+\varepsilon)^{-1}$ and ~30 times lower than $n_{\mathrm{eff}}(\varepsilon_2)$. This indicates that the efficiency of forming transverse crossings using light is about 50 times higher than the efficiency of forming longitudinal bulk transitions by a flow of fast electrons.

Due to the isolation of the three long-wave transition bands 1, 4, 6 in the 3.5–4.7 eV range it is possible to estimate their oscillator strength from the magnitude of the shoulder in $n_{\mathrm{eff}}(\varepsilon_2)$ and $n_{\mathrm{eff}}(-\mathrm{Im}\varepsilon^{-1})$: $f_i \cong 0.012$, 0.018, 0.011 and about 0.0003, 0.0004, 0.0002, respectively.

The second group of bands is in the 5.5–13.0 eV range (Figs. 1b, 1e, 1h, 1k, Table 1). In the reflection spectrum $R(E)$ it consists of eight peaks 9–16, including four narrow peaks 9–11, 13, two very broad bands with a small doublet 12, 14, and a very weak band 16. Their analogues in the calculated spectra $\varepsilon_1(E)$, $n(E)$, and $\sigma(E)$ are shifted to lower energies by about 0.1–0.5 eV

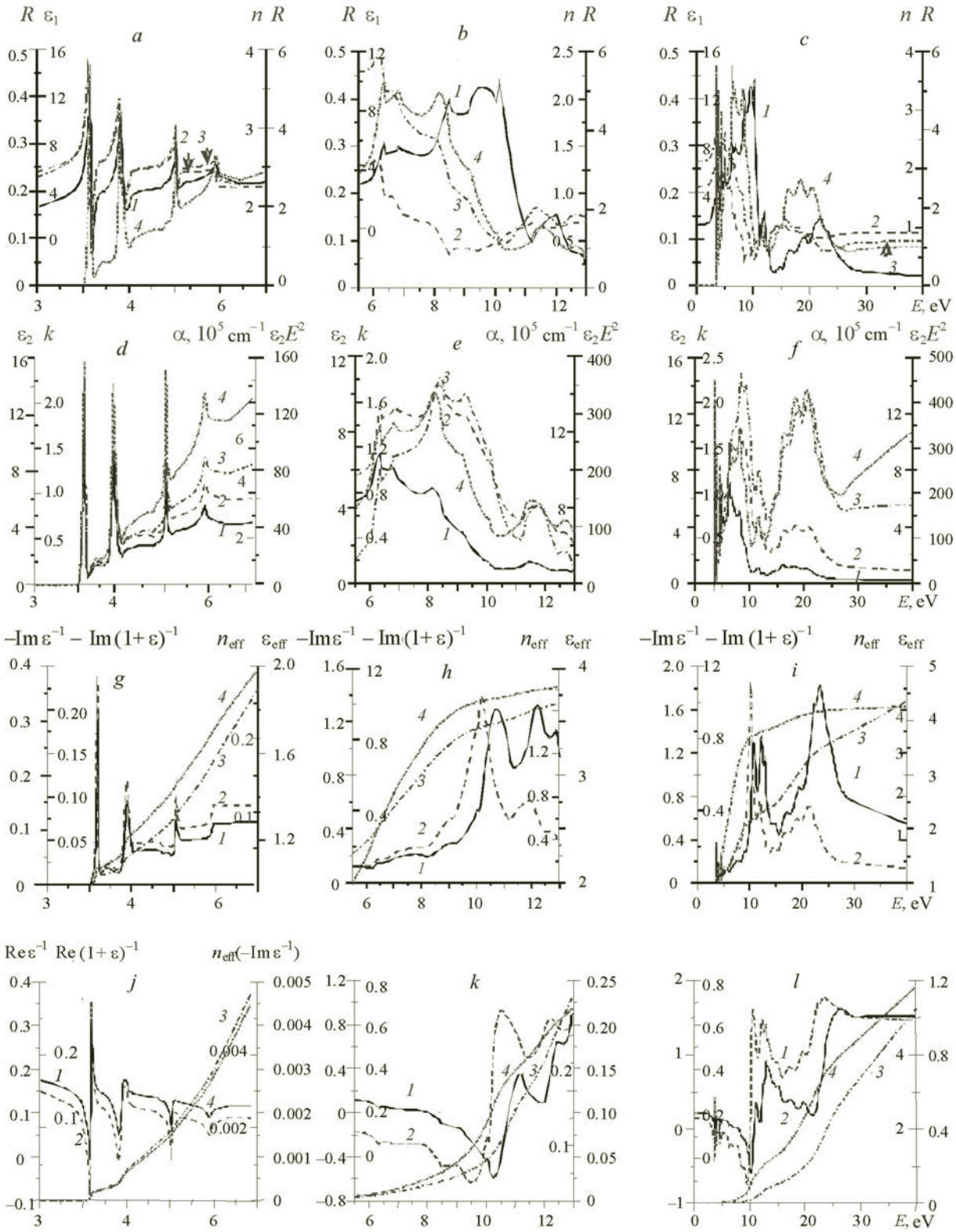

Fig. 1. BaSe crystal spectra calculated based on the experimental $R(E)$ (1) spectrum in the ranges of 3.0–5.5 (a, d, g, j), 5.5–13.0 (b, e, h, k) and 0–40 eV at 77 K (c, f, i, l): a–c) $R(E)$ (1), $\varepsilon_1(E)$ (2), $n(E)$ (3), $\sigma(E)$ (4); d–f) $\varepsilon_2(E)$ (1), $k(E)$ (2), $\alpha(E)$ (3), $E^2\varepsilon_2(E)$ (4); g–i) $-\mathrm{Im}\ \varepsilon^{-1}$ (1), $-\mathrm{Im}\ (1+\varepsilon)^{-1}$ (2), $n_{\mathrm{eff}}(\varepsilon_2)$ (3), $\varepsilon_{\mathrm{eff}}(E)$ (4); j–l) $\mathrm{Re}\ \varepsilon^{-1}$ (1), $\mathrm{Re}\ (1+\varepsilon)^{-1}$ (2), $n_{\mathrm{eff}}(\varepsilon^{-1})$ (3), $n_{\mathrm{eff}}(1+\varepsilon)^{-1}$ (4).

with a relatively strong weakening in the 7.5–10 eV range, a negative value of $\boldsymbol{\varepsilon}_1(E)$ in the 8–11 eV range, and $n < 1$ in the 9.0–13.0 eV range with a valley at about 10 eV ($n \cong 0.5$).

With attenuation of the curves in the range of $E = 9.5$–11 eV analogues of the $\varepsilon_2(E)$, $k(E)$, $\alpha(E)$, and $E^2\varepsilon_2(E)$ spectra hardly shifted as compared to $R(E)$ with the exception of the $\varepsilon_2(E)$ curve with its traditional monotonic intensity decrease observed with increasing energy. Analogues of features of the transverse spectrum $\varepsilon_2(E)$ in longitudinal functions $-\mathrm{Im}\,\varepsilon^{-1}$ and $-\mathrm{Im}\,(1+\varepsilon)^{-1}$ are significantly attenuated with the exception of dramatically increased intensity of features in the 11–13 eV range. In addition to all the transverse features the spectra of the longitudinal functions contain very intense broad peaks E_{p1} (Table 1, Fig. 1h) at about 10.74 ($-\mathrm{Im}\,\varepsilon^{-1}$) and 10.14 eV ($-\mathrm{Im}\,(1+\varepsilon)^{-1}$). They are located at the sharp shortwave decreases of the $R(E)$, $k(E)$, $\alpha(E)$, and $E^2\varepsilon_2(E)$ curves, which is characteristic of plasmon bands formed by the valence electrons of the upper group of occupied energy bands, separated from the lower group of occupied bands. This effect of manifestation of the low-frequency group of bulk and surface plasmons in other cubic crystals is not observed, including in $A^{II}B^{VI}$ crystals, and appears frequently in highly anisotropic compounds [13].

The $\mathrm{Re}\,\varepsilon^{-1}$ and $\mathrm{Re}\,(1+\varepsilon)^{-1}$ spectra basically repeat the $-\mathrm{Im}\,\varepsilon^{-1}$ and $-\mathrm{Im}\,(1+\varepsilon)^{-1}$ curves in the 6.0–9.5 eV range not only in shape but also in structure at the same energies. Their intensities in the 9.5–13.0 eV range increase sharply, and the maxima are shifted to higher energies of shortwave decreases of $-\mathrm{Im}\,\varepsilon^{-1}$ and $-\mathrm{Im}\,(1+\varepsilon)^{-1}$ (Fig. 1k).

With increasing energy the $n_{\mathrm{eff}}(E)$ function linearly increases sharply in the 6–10 eV region from about 0.25 to about 1.4, and continues to slowly climb through 13 eV increasing by $\Delta n_{\mathrm{eff}} \cong 0.25$ to about 1.65 (Fig. 1h). The nature of participation of the valence electrons in the formation of transverse bands in $\boldsymbol{\varepsilon}_2(E)$, $k(E)$ and longitudinal bands in $-\mathrm{Im}\,\varepsilon^{-1}$, $-\mathrm{Im}\,(1+\varepsilon)^{-1}$ is clearly seen from the $n_{\mathrm{eff}}(E)$ spectra calculated from the curves of these four functions (Figs. 1j–1l). The number of valence electrons participating in the formation of the curve of bulk electron energy loss $-\mathrm{Im}\,\varepsilon^{-1}$, in the 5.5–13.0 eV range is mainly about 2 times greater than the data for the surface energy losses $-\mathrm{Im}\,\varepsilon^{-1}$, and is about 20 and 7 times lower in the 6.0–8.5 eV range and at ~10.5 eV, respectively, compared with $n_{\mathrm{eff}}(\varepsilon_2)$. This indicates that the excitation of transverse transition bands by light in the 6–13 eV range is about 10–20 times more efficient than the formation of longitudinal transition bands by a beam of fast electrons.

The third group of the experimental reflectance spectrum bands in the 13–40 eV region is comprised of the four weakest peaks 18–21 and two shoulders 17, 22 (Fig. 1c, Table 1). Their analogues in $\varepsilon_1(E)$ and $n(E)$ spectra are weak and shifted to lower energies by about 0.2–2.0 eV. The curve $n(E)$ in the 30–40 eV range is almost constant at 0.8, is in good agreement with the rule of sums of the expected value of $n(E)$ at high energies and is less than unity. This demonstrates accuracy of the calculations of the spectra of the optical functions of barium selenide.

Analogues of $R(E)$ in the $\varepsilon_2(E)$, $k(E)$, $\alpha(E)$, $\sigma(E)$, and $E^2\varepsilon_2(E)$ spectra occur nearly at the same energies (Figs. 1c, 1f, Table 1). Traditionally, for crystals the curves of $\varepsilon_2(E)$ and $k(E)$ in the weak reflection region are also significantly weakened, especially the $\varepsilon_2(E)$. However, the maxima of the absorption coefficient $\alpha(E)$, the optical conductivity $\sigma(E)$, and the function of the combined density of states $E^2\varepsilon_2(E)$ are quite intense. The highest values of ~0.15 (R, 21), 1 (ε_1, 18), 1 (n, 19), and 1.5 (ε_2), 0.6 (k), $1.2\cdot10^6$ cm^{-1} (α), 400 ($E^2\varepsilon_2$), $2.8\cdot10^{15}$ s^{-1} (σ) are in the 18–21 eV region.

In the calculated spectra of $-\mathrm{Im}\,\varepsilon^{-1}$ and $-\mathrm{Im}\,(1+\varepsilon)^{-1}$ plasmon bands are observed at ~23.3 and 21.3 eV (Figs. 1i, 1l, Table 1), as well as longitudinal analogues of transverse peaks of $\varepsilon_2(E)$ with small (~0.1 eV) and large (~0.4–2.0 eV) longitudinal-transverse splitting energies ΔE_{lt} for the bands 17–19, 22, and 20, 21.

Typically, the valence bands of cubic crystals are not divided into separate groups. Therefore, they are characterized by a common plasmon band. Clear separation of the valence bands into two separate non-overlapping groups is characteristic of anisotropic crystals. For example, for layered materials two groups of valence bands are observed forming two plasmon bands. A similar effect may be observed in BaSe (Fig. 1, Table 1, E_{p1}, E_{p2}). It is interesting to note that with increasing energy the curves of $R(E)$ and $\varepsilon_2(E)$ for BaSe at E_{pv1} decrease sharply, which is characteristic for the plasmon manifestation region. According to our calculations and theoretical results [11], the $\varepsilon_2(E)$ spectrum of BaSe consists of two broad peaks in the 3.5–11.0 and 12–23 eV ranges with shortwave boundaries near E_{p1} and E_{p2}.

Analogues of the $\mathrm{Re}\,\varepsilon^{-1}$ and $\mathrm{Re}\,(1+\varepsilon)^{-1}$ functions in the 13–30 eV region are shifted to higher energies with respect to the $-\mathrm{Im}\,\varepsilon^{-1}$ and $-\mathrm{Im}\,(1+\varepsilon)^{-1}$ spectra by about 0.2 – 0.3 eV (18, 19) or are almost not shifted (20, 21) (Table 1). After the plasmon band the functions $-\mathrm{Im}\,\varepsilon^{-1}$ and $-\mathrm{Im}\,(1+\varepsilon)^{-1}$ decrease rapidly, and the real parts of the functions $1/\varepsilon$ and $1/(1+\varepsilon)$ drop slightly and do not change further until 40 eV.

The effective permittivity $\varepsilon_{\mathrm{eff}}(E)$ curve reaches saturation at a level of 4.25 in the energy range of 20–40 eV, which agrees well with the experimental data $\varepsilon_\infty \approx 4.4$ [8] indicating accuracy of calculations of the spectra of optical functions of the BaSe crystal.

Spectral curves of the effective number of valence electrons $n_{eff}(E)$ involved in the transitions to a given energy E were calculated in the energy range up to 60 eV from the $\varepsilon_2(E)$, $k(E)$, $-\mathrm{Im}\,\varepsilon^{-1}$, $-\mathrm{Im}\,(1+\varepsilon)^{-1}$ spectra. Pairs of curves $n_{eff}(\varepsilon_2)$, $n_{eff}(k)$ and $n_{eff}(-\mathrm{Im}\,\varepsilon^{-1})$, $n_{eff}(-\mathrm{Im}\,(1+\varepsilon)^{-1})$ are almost parallel in the 20–60 eV energy range, i.e. they change in the same way for the transversal functions, but vary greatly with a large slope for the curve $n_{eff}(-\mathrm{Im}\,(1+\varepsilon)^{-1})$. At 15, 25, and 60 eV the values of $n_{eff}(\varepsilon_2)$ are about 10, 4 and 2 times greater than $n_{eff}(-\mathrm{Im}\,\varepsilon^{-1})$, and about 6.7, 3, and 4 times greater than $n_{eff}(-\mathrm{Im}\,(1+\varepsilon)^{-1})$, respectively. Thus, the efficiency of formation of transverse transition bands by light in the 13–25 eV range compared with longitudinal bands is 4–10 times greater, but this difference is reduced twofold when the energy is increased up to about 60 eV.

The peaks 1, 3, 6, and 8 are due to excitons. The distances between the $\varepsilon_2(E)$ peaks 1 and 3 as well as 6 and 8 are about 0.33 and 0.43 eV. For cubic selenides of group II–VI crystals theoretically and experimentally for the exciton line spectra it was determined that both series are due to the spin-orbital splitting of the top valence band at the point Γ by $\Delta_{CO} \cong 0.4$ eV [15]. Therefore, in [5] it is suggested that the shortwave doublet 6, 8 of BaSe is also associated with the main exciton bands at the point Γ. According to theoretical calculations of BaSe bands [9, 10], $E_{gd}(X) < E_{gd}(\Gamma) < E_{gd}(L)$, unlike for group II-VI crystals, for which $E_{gd}(\Gamma) < E_{gd}(L) < E_{gd}(X)$ [15].

According to theoretical calculations [9, 10], in the energy range of $E > E_{gd}(\Gamma)$ the top five or six conduction bands are almost parallel to the top valence band in the directions Γ*L*, *LX*, and *XW*. It is generally accepted that such features contribute to the formation of interband transition peaks accompanied by an exciton band [13]. After two pairs of long-wavelength exciton-type peaks 1, 3 and 6, 8 there is another pair of peaks 9, 10 with the splitting $\Delta E \cong 0.46$ eV, which coincides with the doublet pair 6, 8. We can therefore assume that the $\varepsilon_2(E)$ peaks 9, 10 are also of exciton nature due to near parallelism of the upper conduction bands and upper valence bands at the points in the Γ*X* direction.

Theoretical $R(E)$ spectra obtained without taking into account excitons [9] in the 0–25 eV range, and $\varepsilon_2(E)$ taking into account the excitons in the longwave region [10] are markedly different from the experimental data [5, 6] in structure, in peak position, and relative peak intensities, in addition to strong elevation of the entire $R(E)$ curve and a very large broadening of all exciton bands of $\varepsilon_2(E)$ in the energy range of $E < 5$ eV.

Conclusions. The spectra of the complex of 18 optical fundamental functions of barium selenide crystal in the 0–40 eV range were determined, instead of the known experimental reflectance spectrum. They contain 22 peaks and shoulders present due to excitons and interband transitions, which is 4–5 times greater than in other semiconductors with a cubic crystal lattice. This information can be used to quantify and analyze in detail the theoretical calculations of bands and excitons of BaSe and related crystals in a broad energy range.

Acknowledgment. This work was partially supported by the Russian Foundation for Basic Research programs Nos. 11-02-07038, 12-02-07007.

REFERENCES

1. S. Singh, S. P. Lochab, R. Kumar, and N. Singh, *Chalcogenide Lett.*, **7**, No. 7, 497–500 (2010).
2. N. A. Okereke and A. J. Expunobi, *Chalcogenide Lett.*, **8**, No. 1, 9–14 (2011).
3. R. J. Zollweg, *Phys. Rev.*, **111**, No. 1, 113–119 (1958).
4. G. A. Saum and E. B. Hensley, *Phys. Rev.*, **113**, No. 4, 1019–1022 (1959).
5. Y. Kaneko and T. Koda, *J. Crystal Growth*, **86**, Nos. 1–4, 72–78 (1988).
6. Y. Kaneko, K. Morimoto, and T. Koda, *J. Phys. Soc. Jpn*, **52**, No. 12, 4385–4396 (1983).
7. Y. Kaneko, K. Morimoto, and T. Koda, *J. Phys. Soc. Jpn*, **51**, No. 7, 2247–2254 (1982).
8. J. M. Boswarva, *Phys. Rev. B*, **1**, No. 4, 1698–1701 (1970).
9. A. Pourghazi and M. Dadsetani, *Physica B*, **370**, No. 1, 35–45 (2005).
10. H. Nejatipour and M. Dadsetani, *Phys. Scr.*, **90**, No. 8, 085802(16) (2015).
11. A. Riefer, F. Fuchs, C. R. Rodl, A. Schleife, and F. Bechstedt, *Phys. Rev. B*, **84**, No. 7, 075218(1–13) (2011).
12. V. V. Sobolev and V. V. Nemoshkalenko, *Methods of Computational Physics in Solid State Theory. The Electronic Structure of Semiconductors* [in Russian], Naukova Dumka, Kiev (1988)
13. V. V. Sobolev, *Optical Properties and Electronic Structure of Non-Metals. I. Introduction to Theory* [in Russian], Institute of Computer Science, Moscow, Izhevsk (2012).
14. V. V. Sobolev and V. V. Nemoshkalenko, *The Electronic Structure of Solids in the Region of the Fundamental Absorption Edge. I. Introduction to the theory* [in Russian], Naukova Dumka, Kiev (1992).
15. V. V. Sobolev and V. Val. Sobolev, *Electronic Structure of Solids in the Region of the Fundamental Absorption Edge. II. Crystals of the Group II-VI* [in Russian], Institute of Computer Science, Moscow, Izhevsk (2012).

16. V. V. Sobolev, *Optical Properties and Electronic Structure of Non-Metals. II. Simulation of Integrated Spectra by Elementary Bands* [in Russian], Institute of Computer Science, Moscow, Izhevsk (2012).
17. V. Val. Sobolev and V. V. Sobolev, *Semiconduct. Semimet.*, **79**, 201–228 (2004).
18. V. V. Sobolev, D. O. Mirdas, and V. Val. Sobolev, *Zh. Prikl. Spektrosk.*, **70**, No. 6, 854–857 (2003). [V. V. Sobolev, D. O. Mirdas, and V. Val. Sobolev, *J. Appl. Spectrosc.*, **70**, No. 6, 965–971 (2003)]
19. D. A. Merzlyakov, V. V. Sobolev, and V. Val. Sobolev, *Proc. of the IX Int. Conf. "Amorphous and Microcrystalline Semiconductors"* [in Russian], St. Petersburg Polytechnic University Press, (2014), pp. 372–373.
20. V. V. Sobolev, D. A. Perevoshchikov, D. A. Merzlyakov, V. Val. Sobolev, D. V. Anisimov, and E. A. Antonov, *Proc. of the X Int. Conf. "Amorphous and Microcrystalline Semiconductors"* [in Russian], St. Petersburg Polytechnic University Press, (2016), pp. 119–120.